

IMPURITY BEHAVIOUR IN X-POINT PLASMAS ON JET

B Denne, K Behringer, A Boileau, G Fussmann⁺, M v Hellermann,
L Horton, J Ramette*, B Saoutic*, M F Stamp and G Tallents

JET Joint Undertaking, Abingdon, OX14 3EA, UK

⁺ IPP-Garching, D-8046, FRG

* EURATOM-CEA Association, CEN Cadarache, France

INTRODUCTION

The magnetic separatrix (X-point) configuration has been successfully established in JET /1/. Spectroscopic diagnostics (XUV, VUV, visible and Charge Exchange Recombination Spectroscopy (CXRS)) have been used for studying impurity behaviour in these discharges.

The main impurities in JET plasmas are carbon (from carbon limiters and protection plates) and oxygen. Metals (nickel and chromium from Inconel walls and antenna screens) generally contribute little to Z_{eff} and radiated power. Typical impurity concentrations (in % of the electron density, n_e) are 1/2: 2-4% C, \approx 1% O, and 0.02%, or less, metals. During the period in which most of the X-point operation was carried out, the oxygen concentration in the plasma was, however, somewhat higher (\approx 2%) due to occasional leaks.

X-POINT PLASMAS WITH OHMIC HEATING

During ohmic X-point operation, the carbon concentration was observed to be only 1-2% n_e , a reduction compared to similar limiter discharges, implying that less carbon was produced at the X-point graphite target plates than at the limiters. Metal concentrations were reduced, too, although the plates were most likely covered by wall material. During previous operation with Inconel target plates no increase was observed in metal concentrations in the plasma when changing from carbon inner-wall to X-point operation. These observations indicate a low plasma temperature (\approx 20 eV) in front of the plates, resulting in a low sputtering yield. The oxygen concentration, oxygen most likely originating from the vessel walls, was 1-2% n_e , similar to limiter plasmas for the same plasma conditions. As a result, for given \bar{n}_e , Z_{eff} was somewhat lower in X-point as compared to limiter plasmas (see Fig.1). The total power radiated, P_{rad} , was \approx 40% of the input power at the lowest electron densities, increasing with n_e and approaching 100% at $\bar{n}_e = 2 \times 10^{19} \text{ m}^{-3}$. This includes the power radiated from the X-point region which was 30-40% of the total power radiated in all cases.

ADDITIONAL HEATING (L-MODE)

During additional heating a modest increase in n_e was observed. With Neutral Beam Injection (NBI) both carbon and metal concentrations were higher than in the ohmic case, which is consistent with an observed increase in the edge electron temperature, although the metals might also have originated from CX sputtering. The C/O ratio increased during NBI, in contrast to what was observed in limiter plasmas, where oxygen was the dominant impurity during NBI at high \bar{n}_e . Somewhat higher Z_{eff} -values were found in X-point plasmas with additional heating - the general

falling trend with increasing n_e , observed in ohmic cases, being maintained. During Ion Cyclotron Resonance Heating (ICRH) and combined heating, increased levels of screen material (Ni and Cr) were found in the plasma as in the limiter cases /2/. The total power radiated from the bulk of the plasma was typically -25% of the total input power.

H-MODE

During H-mode, n_e increased steeply (Fig.2). The electron density profile was quite flat. Langmuir-probe data /3/ showed that n_e in the scrape-off layer was approximately constant throughout the duration of the H-mode despite -3x increase in bulk density. The electron temperature profile became broader and the edge temperature was high (a few 100 eV). Radiation emitted from peripheral carbon and oxygen ions (C III - C V and O IV - O VII lines) was essentially unchanged (or even decreased) after the L-H transition, whereas C VI and O VIII radiation, emitted from radial locations further in, increased, reflecting the increasing bulk electron density. The behaviour of the lowly-ionised C and O is consistent with the observed change in edge parameters, and results in less total radiation per ion for these light impurities. After the H-mode was established, the total power radiated from the bulk plasma increased approximately as \bar{n}_e^2 /4/, except when ICRF was applied, in which case it increased more steeply due to some metal contribution. Eventually the radiation losses lead to the termination of the H-mode. No ASDEX-type edge-localised-modes (ELM's) (see e.g./5/) were observed, probably because of the high radiation levels.

The bulk particle confinement increased by a factor -3 /6/ in the L-H transition. The impurity confinement increased similarly. For carbon the improved confinement can be seen in Fig.2: the carbon concentration is essentially constant, or increases slightly in the H-mode, although the carbon influx (represented by the C III-line brightness) remains unchanged with respect to the hydrogen flux, ϕ_H (carbon production yield $\phi_C/\phi_H=5\%$). Towards the end of the H-mode the impurity confinement deteriorated as τ_E (deduced from the decay of the nickel concentration). There is no indication of impurity accumulation in the neoclassical sense. Analysis of several metal ionisation stages as well as the soft X-ray emission profiles and bolometer profiles show that the metal density profile is not peaked. The absence of impurity accumulation might be explained by the presence of sawteeth in the H-mode discharges.

The bolometer profiles are hollow with a broad radiating shell /4/. Transport code modelling for carbon and oxygen reproduces the measured peak radiated power, but the measured radiating shell extends further in radially than predicted by the code. This discrepancy is presently not understood.

During the H-mode, Z_{eff} did not decrease as normal at high \bar{n}_e (see Fig.1), but remained similar to the lower- \bar{n}_e values of 3-4. The high Z_{eff} values could be accounted for by the measured central concentrations of light impurities. The C/O ratio during H-mode was 1-2:1. An observed increase in metal density can be explained either by sputtering by CX neutrals or by the increased edge temperature. The metal concentration is rather independent of n_e for H-mode plasmas which contrasts with the falling trend with increasing \bar{n}_e seen in all other types of discharges.

However, the metal concentration is still low: its contribution to Z_{eff} is ≤ 0.2 , and $\leq 10\%$ of P_{rad} is due to metals according to transport code calculations. For the discharge shown in Fig.2, e.g., the metal concentration at the end of the H-mode was 0.002%.

SUMMARY AND CONCLUSIONS

In ohmic X-point plasmas Z_{eff} is reduced somewhat compared to similar limiter discharges as a result of lower carbon and metal concentrations. This indicates a low plasma temperature in front of the neutraliser plates.

In additionally heated, L-mode, X-point plasmas, carbon and metal concentrations are higher, consistent with the observed increase in edge temperature. ICRH and combined heating results in higher levels of screen material (Ni and Cr) in the plasma like in the limiter cases.

During H-mode, particle confinement improves by a factor of ~ 3 ; impurity confinement improves similarly. No impurity accumulation, in the neoclassical sense, has been observed.

During H-mode, Z_{eff} does not decrease as normal with higher \bar{n}_e , but remains at values of 3-4, typical of lower- \bar{n}_e plasmas. Measured carbon and oxygen concentrations (from CXRS) can account for the measured bulk radiated power and Z_{eff} , metals contributing only little.

No ASDEX-type ELM's have been observed. ELM's could allow control of the plasma density and impurity contamination. It might be possible to achieve longer H-modes in JET by reducing the impurity content of the plasma, in order to obtain ELM's, or to provide some efficient density pumping mechanism.

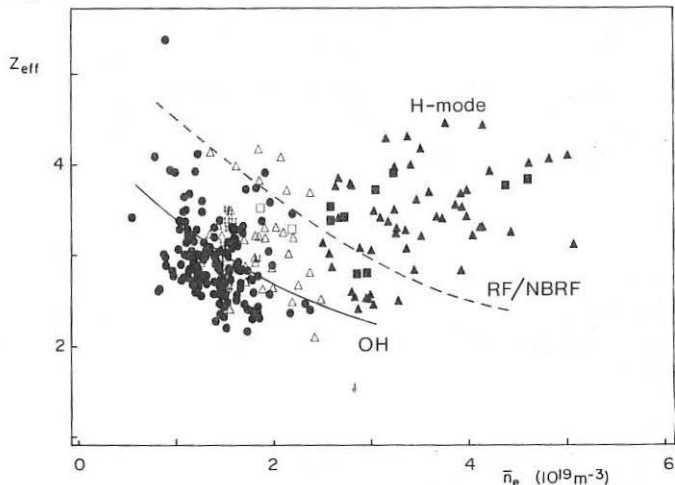


FIG.1 Z_{eff} vs \bar{n}_e for X-point plasmas with ohmic heating (●), NB-heating (Δ) and combined heating (■) (filled symbols denoting H-mode). For comparison the typical behaviour of limiter plasmas with ohmic heating (—) and with RF/combined heating (----) are shown.

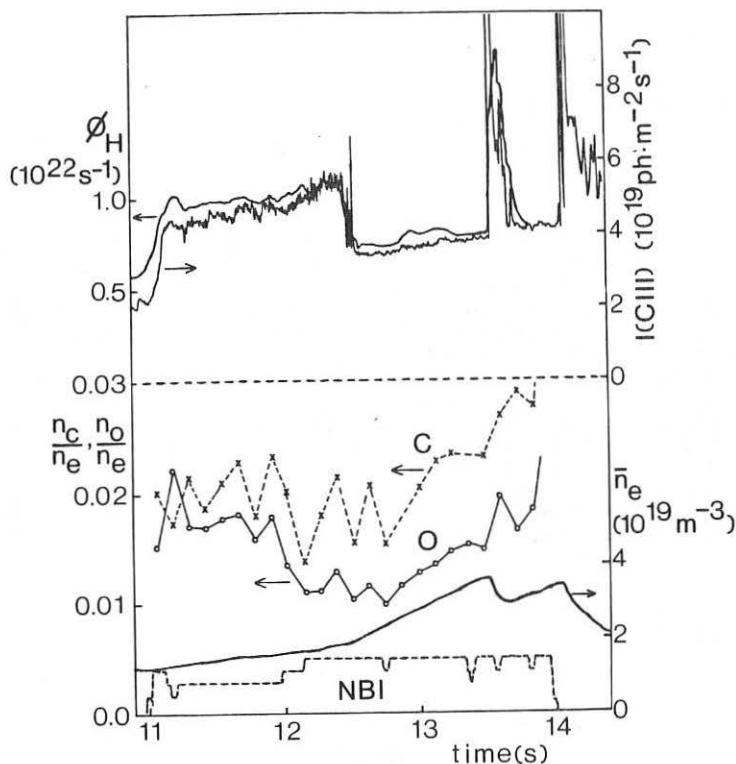


FIG.2. Behaviour of line average electron density (\bar{n}_e), carbon and oxygen concentrations (from CXRS), hydrogen flux (ϕ_H), and carbon influx, represented by the brightness of a C III-line (vertical viewing) during L- and H-mode in a NB-heated (5MW) X-point discharge. The L+H transition takes place at -12.5 s.

REFERENCES

- [1] Keilhacker, M, et al, (this conference)
- [2] Behringer, K et al, IAEA, Kyoto 1986
- [3] Tagle, A J (private communication)
- [4] Jäckel, H, et al (this conference)
- [5] Keilhacker, M, et al, Plasma Phys.and Contr.Fusion 26, 49(1984)
- [6] Morgan, P D and O'Rourke, J J, (this conference)